Tellus (2007), 59A, 114–121
Printed in Singapore. All rights reserved

TELLUS

On precursors of South American cyclogenesis

By DAVID MENDES[1]*, ENIO P. SOUZA[2], ISABEL F. TRIGO[3] and PEDRO M. A. MIRANDA[4], [1]*Centro de Geofísica da Universidade de Lisboa, Faculdade de ciências, Departamento de Física, Campo Grande, Ed. C8, Piso 6, 1749-016 Lisboa, Portugal;* [2]*Federal University of Campina Grande, Department of Atmospheric Sciences, Campina Grande, Brazil;* [3]*Meteorology Institute of Portugal, University of Lisboa, CGUL, IDL, Lisboa, Portugal;* [4]*University of Lisbon, CGUL, IDL, Lisboa, Portugal*

(Manuscript received 28 October 2005; in final form 5 October 2006)

ABSTRACT

Cyclogenesis over the southern region of South America is studied in relation to the evolution of dynamic and thermodynamic fields over the continent, using storm tracking and derived composite analysis over a 25 yr period. Results show that, irrespective of the season, there is always a moist-entropy reservoir northwest of the cyclone formation region. One day before cyclone formation, moist entropy over North Argentina is anomalously high and increasing, due to an intensification of the northerly flow along the eastern flank of the Andes, peaking at the time of cyclogenesis. The new cyclone is fed by warm and moist air coming from the continent but, as it intensifies and moves eastwards, imposes an anomalously southerly flow reducing the moist-entropy anomaly over South America. The presence of the Andes Cordillera plays a major role controlling the location of the main cyclone formation area in the region by (i) channelling the warm moist northerly flow in the lower troposphere and (ii) inducing cyclonic circulation in the lee side, when upper troughs travelling eastwards move over the mountain range at the middle latitudes.

1. Introduction

Extratropical cyclones play a central role in the maintenance of global climate and are responsible for the transport of heat and moisture through the troposphere (Peixoto and Oort, 1992; Simmonds and Keay, 2000). The South Atlantic is one of the regions of the globe where cyclones preferably occur. According to Frederiksen (1985), the observed location of the primary storm track just downstream and polewards of the polar jet stream in the Southern Hemisphere is accounted for by linear baroclinic instability theory. However, James and Anderson (1984), using one of the first years of analysed data for the Southern Hemisphere provided by the European Centre for Medium-range Weather Forecasts (ECMWF), found that the linear dry baroclinic theory was unable to explain the observed storm track in the South Atlantic sector. At the same time, these authors noted the anomalous low-level wind field over the South American continent, with a strong mean north–south flow east of the Andes Mountains. Such flow could imply an extra source for cyclogenesis, through moisture entrainment into the low-level westerlies at mid-latitudes, downstream of the source in the Amazon basin.

Gan and Rao (1991) showed that cyclone formation in South America is mostly associated with baroclinic instability. In addition, they pointed out the importance of topographical effects caused by the presence of the Andes Mountains. Furthermore, Garreaud and Wallace (1998) found that transient incursions of mid-latitude air into subtropical and tropical South America, east of the Andes, are an important feature of the synoptic climatology over this region, associated with the enhancement of convection.

This study puts into evidence the conditions, which favour the onset and intensification of cyclones in the region of maximum cyclogenesis near South America. It will be shown that events of low-level cyclogenesis are preceded by an increase in the spatial heterogeneity of the moist-entropy field, with the building up of warm and moist air over a preferred South American region, to the North of Argentina. There, cyclogenesis events tend to occur when an upper-level trough crosses the Andes, favouring the generation of cyclonic relative vorticity in the lee side. The low-level warm and moist air that sits over the continent, near 30°S,60°W, is then advected into the new cyclone, contributing for its development.

2. Data and methodology

The data used here consist of the following 6 hr fields, on a 2.5° × 2.5° regular grid: sea level pressure (SLP); 500 hPa geopotential

*Corresponding author.
e-mail: dmendes@fc.ul.pt
DOI: 10.1111/j.1600-0870.2006.00215.x

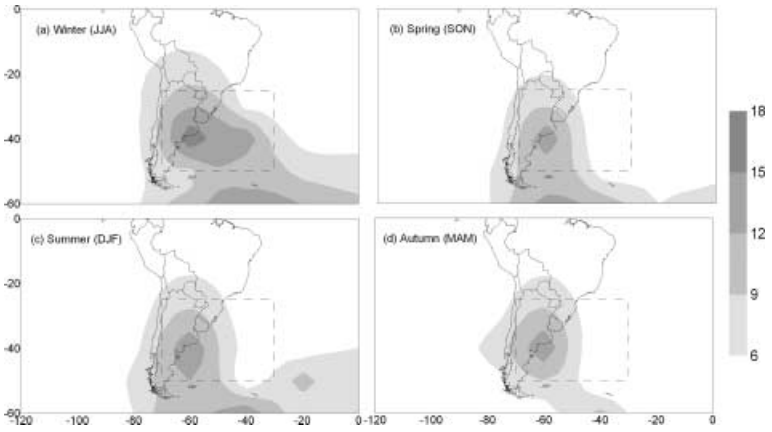

Fig. 1. Frequency of cyclogenesis near South America: mean number of events per season in each 7.5° × 7.5° box. The dashed rectangle delimits the region of cyclogenesis used to compute the composite means and histograms in the following Figs. 3–8. Computed from NCEP reanalysis 1979–2003.

height (Z500); 850 hPa horizontal wind; absolute air temperature and relative humidity, both at 1000 and 500 hPa. The data, available from the National Center for Environmental Prediction/National Center for Atmospheric Research (NCEP/NCAR) reanalyses data set (Kalnay et al. 1996), was analysed in the region 120°W–0°, 60°S–0°S, spanning the period from 1979 to 2003.

Cyclones are detected by identifying minimum values in SLP, according to the methodology proposed by Trigo et al. (1999). To be considered a cyclone, these minima must also fulfil an empirical threshold on the mean pressure gradient. In this case, the pressure gradient estimated for an area of 9° lat × 12° long must be at least 0.55 hPa/250 km. The tracking of cyclones, performed over the entire Southern Hemisphere, but only shown in the selected region near South America, is based on the search for the nearest neighbour in the previous chart considering a maximum for cyclone speed of 33 km hr^{-1} in the westward direction and 90 km hr^{-1} in any other. If the nearest neighbouring centre in the previous chart is outside the area defined by those speed thresholds, then cyclogenesis is assumed.

Finally, to avoid taking into the cyclone statistics weak events with little impact on local weather, only centres lasting a minimum of 24 hr, and with a minimum pressure, taken throughout the whole lifecycle, below 1010 hPa (e.g. Gan and Rao, 1991; Dal-Piva, 2001; Trigo 2005) are considered hereafter to be extratropical cyclones.

The thermodynamic state of the systems was analysed through two variables: the equivalent potential temperature (θ_e) and the saturation equivalent potential temperature (θ_e^*). A detailed description of the calculation of these variables is given by Bolton (1980). θ_e and θ_e^* can be related with the entropy of moist air through $S = c_p \ln\ \theta_e$ and $S^* = c_p \ln\ \theta_e^*$, respectively (Emanuel, 1989). Therefore, despite the logarithmic relation, θ_e and θ_e^* will be used throughout the text, but one will often refer conceptually to them as moist entropy and saturation moist entropy.

A conditional instability index is used in the following analysis. This is defined as the difference between θ_e at 1000 hPa and θ_e^* at 500 hPa, following Rennó and Ingersol (1996), over the cyclone centre. Next, composite means and/or anomalies of this index as well as of SLP, Z500 and near surface wind will be presented and discussed for situations prior, during and after cyclogenesis occurring in the South American region, within the area (70°W–30°W; 25°S–50°S) shown in (Fig. 1).

3. Results and discussion

Figure 1 shows the seasonal mean number of cyclogenesis near South America. A total of 2609 events were diagnosed, from NCEP/NCAR reanalyses, for the period 1979–2003 in the selected area. Most events occur over the Atlantic Ocean, off the Argentinean coast, with some cases in continental South America over Argentina, Uruguay and South Brazil. This result agrees with previous studies (Gan and Rao, 1991; Sinclair, 1995; Simmonds and Keay 2000). The number and spatial distribution of cyclogenesis events varies between seasons, with higher frequencies in winter and a north–south displacement in the annual cycle.

Figure 2 displays the JJA mean distribution of 850 hPa wind, 1000 hPa θ_e, and θ_e variance. As previously mentioned, it displays important meridional low-level flow on both sides of the Andes Mountains, concentrated around 20°–25°S (15°–20°S) over the American continent in winter (summer). The region of maximum θ_e lies east of the Andes, extending southwards along the northerly warm and moist flow from the Amazon basin, that is, the low-level jet (Marengo et al., 2004), and moves further south in summer (Fig. 2d). The region of maximum θ_e variance is centred near 60°W, to the south of maximum θ_e, positioned between 25°S (in winter) and 32.5°S (in summer), over Argentina. The location of maximum θ_e variance coincides with a region where cyclones and mesoscale convective complexes are frequent (Velasco and Fritsch, 1987; Gan and Rao, 1991; Satyamurty et al., 1998). The high variance over latitudes south of 60°S in winter (Fig. 2a) marks the mean position of the circumpolar winter storm tracks (e.g. Simmonds and Keay, 2000).

The fact that the region of most frequent cyclogenesis (Fig. 1) is located slightly to the south of the region of maximum θ_e

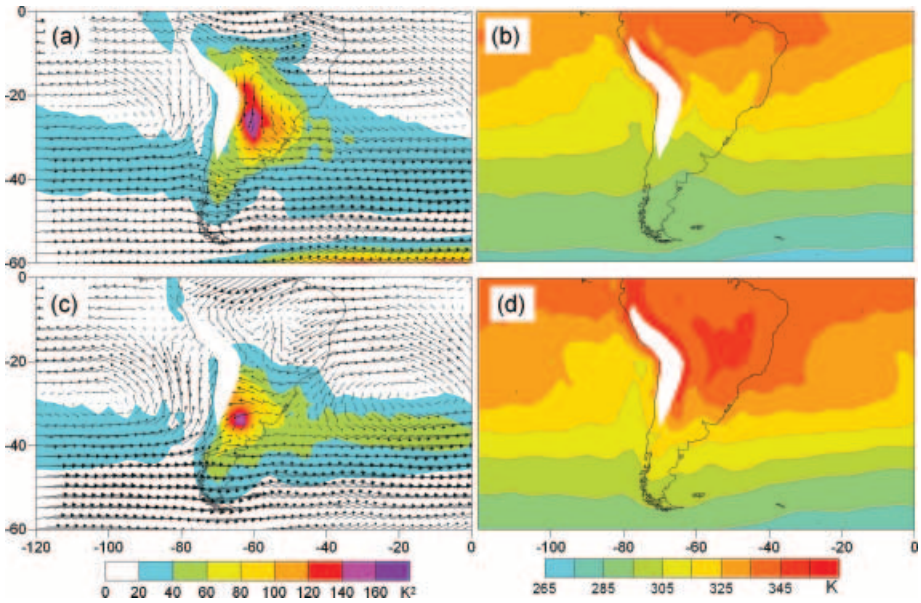

Fig. 2. (a) Variance of θ_e and mean 850 hPa wind in winter (JJA); (b) mean θ_e at 1000 hPa in winter; (c) variance of θ_e and mean 850 hPa wind in summer (DJF) and (d) mean θ_e at 1000 hPa in summer. The maps have been blanked in the regions where the mean topography is above 1500 m.

variance over South America on the lee side of the Andes (shown in Fig. 2 for winter and summer) suggests a link between θ_e anomalies in the continent and the process of cyclogenesis that will now be explored. Figures 3a–f show composite anomalies, with respect to the 1979–2003 winter climatology, of SLP and 500 hPa geopotential height (left panels), and of the 850 hPa mean flow and 1000 hPa θ_e (right panels), corresponding to the pre-storm formation (day -1), cyclogenesis (day 0) and post-storm formation (day $+1$). The composites are computed using the storm-tracking algorithm described above: each cyclogenesis event contributes with one member to the ensemble mean at day -1, day 0 and day $+1$. The regions where composite means are statistically different from the respective season climatology, at less than the 5% significance level, are also indicated in Figs. 3–6; statistical significance was evaluated using a two-tailed Student's *t*-test (e.g. Wilks, 1995). As expected there is a good agreement between the position of SLP minima for day 0 (Figs. 3b, 4b, 5b and 6b) and maxima of cyclogenesis frequency (Fig. 1). The higher dispersion of cyclone events in spring compared to that of autumn (Figs.1b and d) may explain the lower statistical significance observed in the field of SLP anomalies of the former. On the other hand, the high standard deviation of central pressure obtained for cyclones detected for the summer season (not shown) explains the relatively small area with statistical significant SLP anomalies.

Composites of Z500, for the days preceding cyclogenesis in South America, show a moving trough over the southeastern Pacific, approaching the Southern tip of the Andes barrier at day -1 (Fig. 3a). The mean location of the trough aloft, which is generally associated with a travelling low originated over the South Pacific, does not change much throughout the year, being generally within the 40°S–50°S band (Seluchi, 1995).

As the upper perturbation moves over the Andes in the day before cyclone formation, the maximum θ_e anomaly, corresponding to θ_e values statistically warmer than the climatological mean, is centred near 30°S,60°W (Fig. 3d) and intensifies up to 8 K at day 0 (Fig. 3e), in the same location. The build up of positive anomalies of θ_e is likely to increase coastal low-level baroclinicity, further contributing to the location of cyclogenesis maxima near the South American coast. The anomalous wind field at day -1 exhibits enhanced northerly flow over most of the continent, particularly along the eastern flank of the Andes (Fig. 3d) transporting tropical moist air southeastwards into the preferred sector of near surface cyclogenesis. At day 0 (Fig. 3e) the anomalous flow turns to southerly for latitudes south of 25°S in the west part of the continent, intensifying low-level convergence in the region of maximum θ_e anomaly. At day $+1$ the maximum θ_e anomaly is reduced and advected to the ocean (Fig. 3f). At days 0 and $+1$ there is clear evidence of a developing cyclonic circulation near the coast (Figs. 3e and f) superimposed over the area of negative SLP anomalies (Figs. 3b and c), in agreement with Fig. 1.

Results shown in Figs. 2 and 3 suggest that the southward transport of moist entropy from tropical Amazon into the subtropics and to the mid-latitude east coast of South America is a feature clearly associated with cyclogenesis in this sector. More specifically, the composite fields analysed here suggest cyclogenesis over and around South America is generally associated with (i) the accumulation of moist entropy over the continent, by northerly advection from the tropics and (ii) the propagation

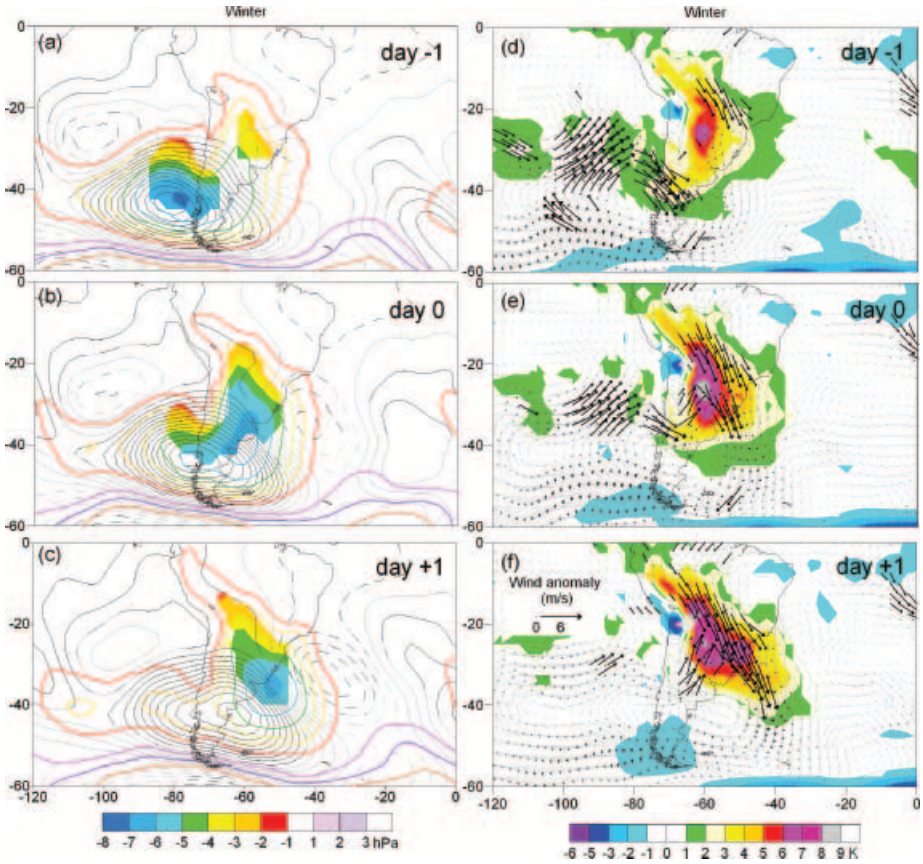

Fig. 3. Composite anomalies corresponding to one day before (day−1), during (day 0), and one day after (day+1) cyclogenesis events detected in Winter (JJA), for the 1979–2003 period. Left: sea level pressure anomaly (colour lines, painted in the areas where the anomalies are statistically significant), and 500 hPa geopotential height (5 m contour, dashed > 0, darker lines are statistically significant). Right: 850 hPa wind anomaly (vectors, darker arrows are statistically significant), θ_e anomaly (colour contours, painted where statistically significant).

of an upper-level trough over the southern tip of the Andes barrier. The latter favours the formation of a cyclonic circulation in the lee side, over the area of enhanced warm moist air near the coast of Argentina, with low-level convergence intensified by an anomalous southerly flow at higher latitudes, over the continent (Fig. 3f). The role of this southerly flow in cyclogenesis events was already noted by Garreaud and Wallace (1998) using a completely different classification technique, which relied on the distribution of outgoing longwave radiation (OLR), instead of the low-level pressure field as used here, for storm detection. The present analysis puts the emphasis on the southward transport of moist entropy over the South American continent, along with the upper moving trough, which seem to be the two main elements in the period of storm formation, while Garreaud and Wallace (1998) stress the importance of the southerly cold air flow into the subtropics. The effects analysed in both studies are important, and the difference in emphasis results from the storm detection technique: the discrepancies can be explained if one accepts that the pressure-based storm-tracking algorithm used here detects the storm formation about one day before its detection by the OLR analysis, more sensitive to cloud formation and thus attaining its peak in a more mature stage of the storm.

Figures 4–6 show the composite anomalies for the other seasons: spring (SON), summer (DJF) and autumn (MAM), respectively. Many of the features mentioned above are present in all seasons, in particular the positive anomalies of θ_e centred near 30°S,60°W and peaking at the time of cyclogenesis. Spring (Fig. 4) composite anomalies are very similar to those shown for winter, although one notices a slightly stronger low-level cold anomaly at days 0 and +1, associated with stronger southerly flow over the southern sector of the continent. This feature is also present in autumn (Fig. 6) and even more strongly in summer (Fig. 5). In the latter season, the upper-level anomaly is much more to the south, and it travels over the (lower) southern tip of the Andes earlier in the cyclogenesis process. The similarities between anomaly fields obtained for the different seasons suggest that similar processes are active throughout the year, in particular the low-level northerly jet in the east flank of the Andes and the southerly flow associated with the newborn storms.

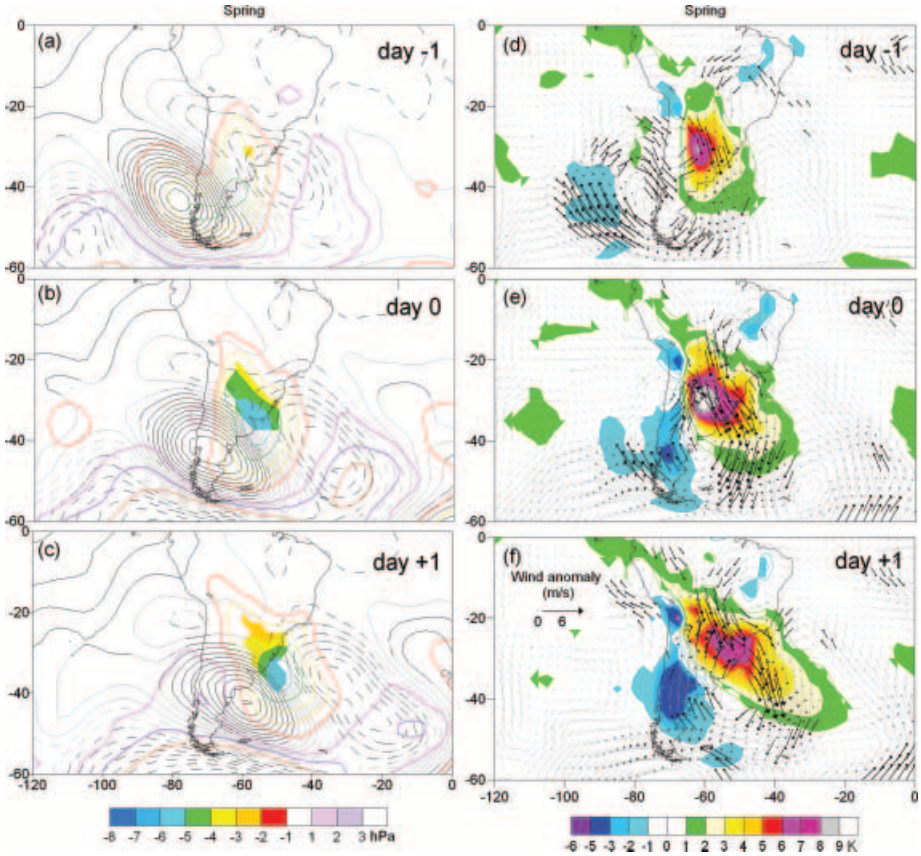

Fig. 4. As Fig. 3 for spring (SON).

The evolution of selected thermodynamic properties during storm development will now be analysed. Figure 7 shows, for each season (JJA, SON, DJF and MAM, respectively), composite means of the evolution of cyclones central pressure (δp), measured as the difference between the cyclone central pressure at time t and at the formation time ($t = 0$), potential temperature anomaly in the region of maximum variance over South America (30°S,60°W), conditional instability index (difference between 1000 hPa equivalent potential temperature $\theta_{e,1000}$ and 500 hPa saturation equivalent potential temperature, $\theta^*_{e,500}$) at the centre of the storm, and finally the analysed precipitation rate, averaged over an area of 2.5° × 2.5° around the cyclone centre. The variables taken at the (moving) cyclone centre (pressure anomaly, conditional instability and precipitation rate) are only available after cyclogenesis. Prior to that time, Fig. 7 shows those variables computed at a fixed point that is the point where cyclogenesis will occur, allowing for an analysis of the pre-storm environment.

It is worth noting the following features present in Fig. 7, for all seasons, namely: (i) the potential temperature anomaly in the region of maximum variance (30°S,60°W) peaks at the cyclone formation time ($t = 0$), while (ii) the conditional instability index ($\theta_{e,1000} - \theta^*_{e,500}$) increases after the formation of the cyclone, peaking in its mature state (36 or 48 hr after cyclogenesis), when SLP attains its minimum; the index presents a clear anti-correlation with central pressure, consistent throughout the whole year and (iii) the analysed precipitation rate peaks slightly earlier than the conditional instability index, except in winter, and, drops off quicker in all seasons.

The histograms shown in Fig. 8 put in perspective the evolution of potential temperature anomalies (in the region of maximum variance), for all cyclogenesis events detected in winter and summer in the South American sector. For both seasons, the evolution of θ_e anomalies confirms the building up of a warm moist air mass in the lower troposphere, which tends to peak at cyclogenesis. The variability among the cyclone population, however, is significantly higher in winter, presenting a rather flat distribution with slightly higher frequencies around the median. This suggests a relatively high variability of patterns in the lower troposphere potential temperature preceding and following cyclogenesis events. In contrast, the summer histograms seem to have two frequency maxima, although the higher frequency one clearly dominates the secondary peak, suggesting the coexistence of two main cyclogenesis types/mechanisms in that season. The dominant one, corresponding to the distribution around the highest peak (the mode), indicates that summer cyclogenesis tends to occur when θ_e anomalies reach values of the order of 8 K (as also depicted in Fig. 7c). Histograms were

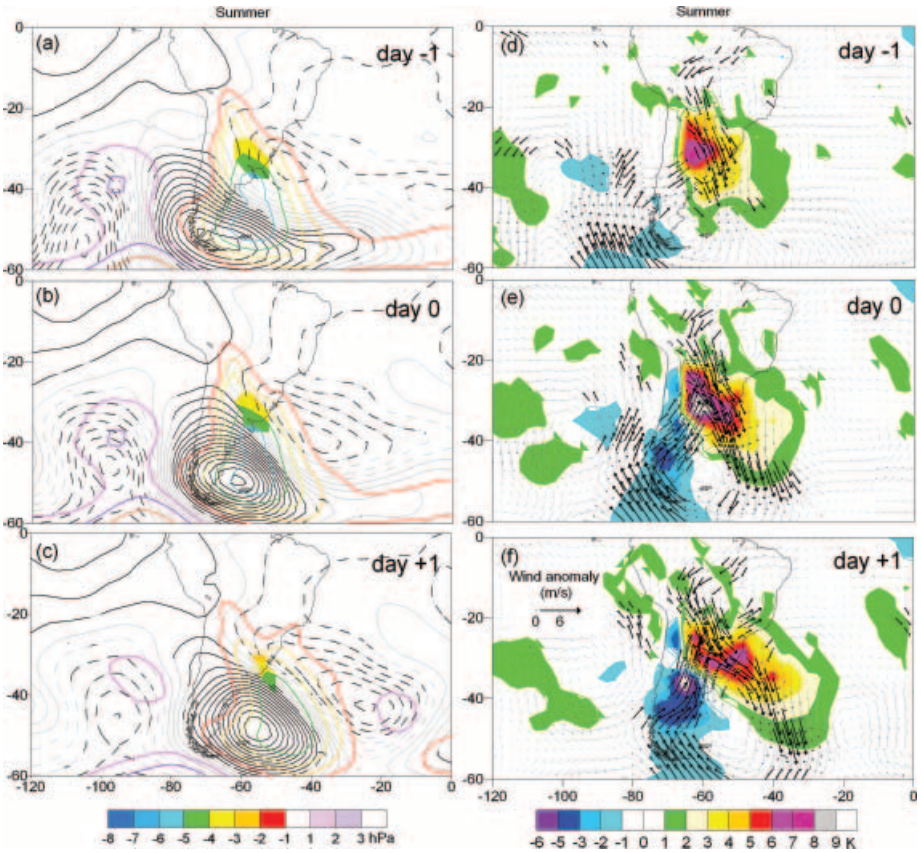

Fig. 5. As Fig. 3 for summer (DJF).

also computed for the other seasons (not shown): the spring histograms are similar to those found for winter, whereas autumn histograms are very close the ones computed for summer.

Precipitation seems to play an important role in the development of the (mean) storm, increasing by a factor of 3 in winter and up to a factor of 9 in summer, and somewhere in between in the other seasons. The maximum rate of precipitation is diagnosed before the maximum low-level deepening, except in winter where the mean precipitation rate is significantly lower. This fact suggests that precipitation also contributes to the deepening of the storm, in agreement with the case studies analysed by Seluchi and Saulo (1998) and Possia (2002). These works go further than the composite analysis presented here, as they suggest that the formation of a low-level cyclone does not occur if precipitation processes are removed.

4. Concluding remarks

This study is focused on the analysis of preconditions for the formation of extratropical cyclones over and around South America. A 25 yr database of extratropical cyclones and respective trajectories, including an average of 112 cyclogenesis events per year, provides a robust climatology, which is characterized by some remarkable features: (i) this large number of events originate from a rather localized area; (ii) the cyclogenesis process is preceded by anomalous flow over the continent, associated with the transport of warm and moist air into the cyclogenesis region and (iii) cyclogenesis occurs in all seasons with similar mean anomalies but somewhat different statistics. In the cyclogenesis process, the Andes Mountains seem to play a dual role: first, by channelling warm and moist tropical air into the mid-latitudes, a process that leads to the building up of positive anomalies of moist entropy over the continent in the pre-cyclogenesis period; later by interacting with upper-level cyclones that travel in the southern Pacific at higher latitudes, and which eventually trigger the new downstream cyclogenesis.

The storm-tracking algorithm used to compute the storm statistics, was the basis of a new composite analysis of the life cycle of South American cyclones, which showed that there is a very clear relation between the phase of the moist-entropy anomaly over the region of maximum variability, and cyclogenesis near South America. During the pre-formation period, when a tendency of pressure lowering in the formation region is already noted, there is an increased convergence of moist air coming from North into Northern Argentina leading to a large positive anomaly in the moist-entropy field (θ_e). On average, this anomaly, located to the northwest of the cyclogenetic region, reaches its maximum at the time of cyclogenesis, for all seasons.

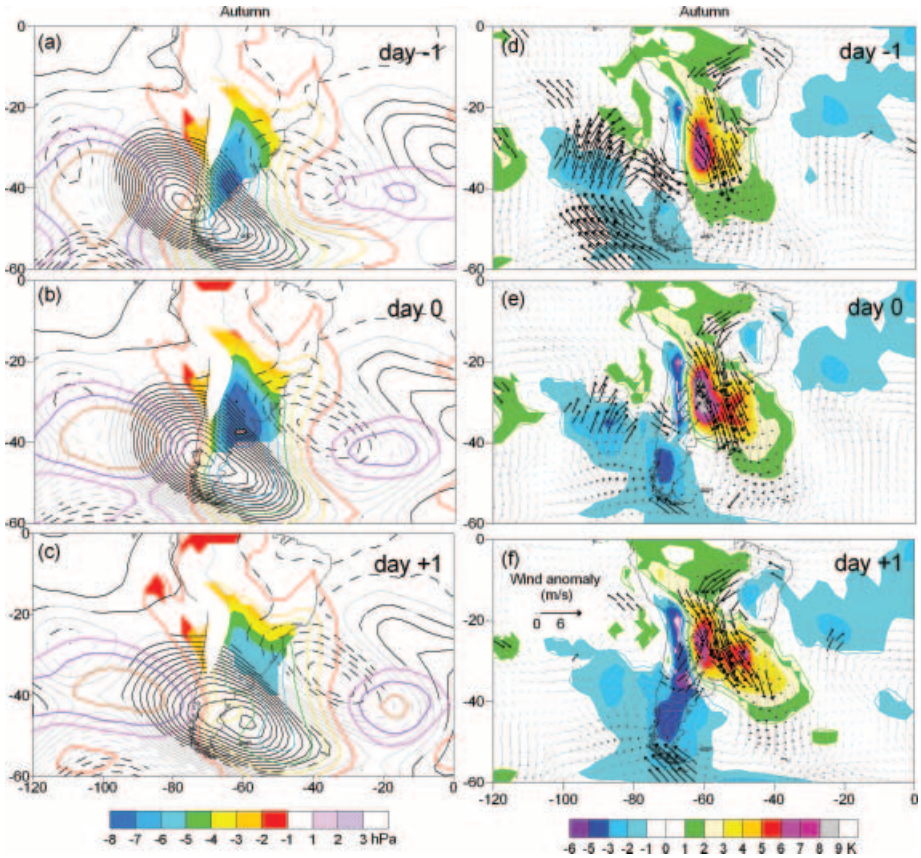

Fig. 6. As Fig. 3 for autumn (MAM).

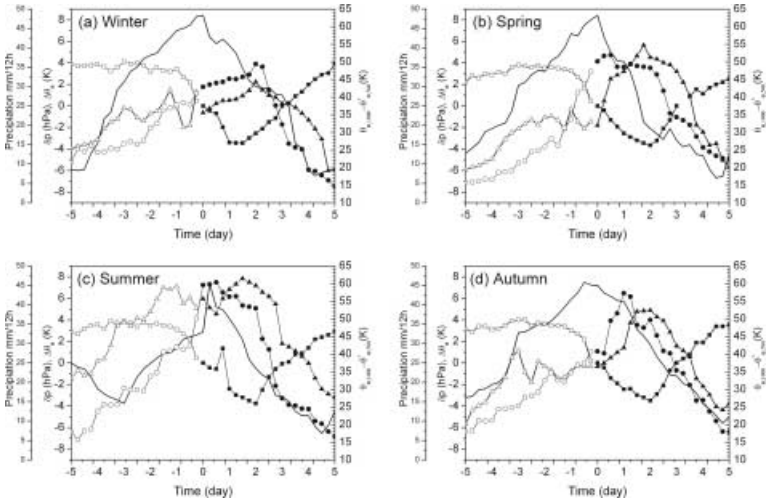

Fig. 7. Composite means of θ_e anomaly at 30°S 60°W (solid line), sea level pressure anomaly at the cyclone centre (squares), conditional instability (triangles), and precipitation, area averaged over a 2.5° × 2.5° cell, in the same location (circles). Pressure, conditional instability and precipitation are computed at the centre of the moving cyclone after cyclogenesis (filled symbols, after day 0), and at the fixed location of the following cyclogenesis (hollow symbols) prior to day 0.

After that time, the anomaly over the continent decays rapidly, as the newly formed cyclone advects the moist air eastwards. However, the cyclone development proceeds with an increase in conditional instability, maintained by the input of moist warm air to the cyclogenetic region from the continent, followed by the release of latent heat due to enhanced precipitation in the core of the storm.

While the moist-entropy anomaly over the continent is always positive at cyclogenesis, its time series present strong variability among the cyclogenesis events in winter, except in summer, when most cyclogenesis occur for values of the anomaly near or above its mean value of +8 K (Fig. 8). This suggests the possibility of different populations of storms in the different seasons, something that will be studied in future work.

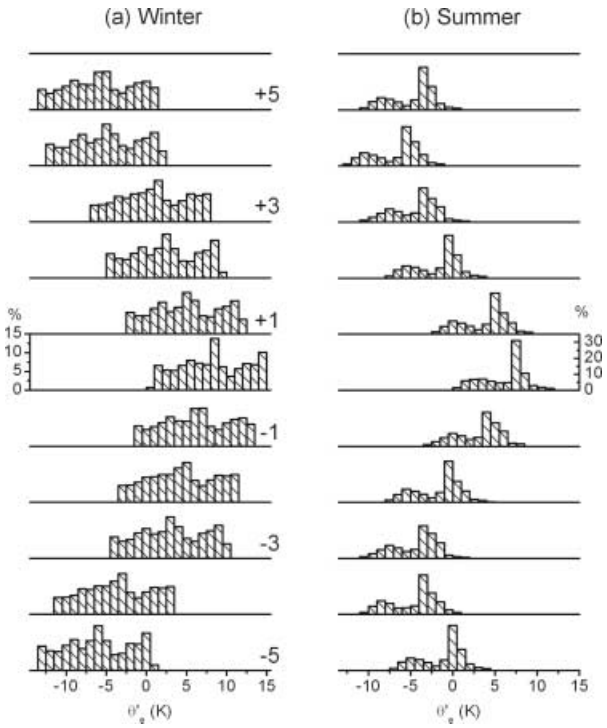

Fig. 8. Frequency distribution of the θ_e anomaly at 30°S,60°W in composite sets of data near cyclogenesis (days −5 to +5, from bottom to top), for winter (JJA; left panel) and summer (DJF; right panel).

The previous results suggest that the mid-latitude cyclones generated in the southern part of South America are largely controlled by interactions between the mid-latitude circulation and the tropics, through north–south flow over the continent, along the east slope of the Andes Mountains, confirming an hypothesis initially proposed by James and Anderson (1984) based on 1 yr of data. The mean circulation in the region, reinforced in the days prior to cyclogenesis, transports moist air from the Amazon basin into east subtropical South America, near 15°S,70°W, very close to the Andes. Cyclogenesis is accompanied by the transport of that low-level warm and moist air into the cyclone, increasing conditional instability and leading to cyclone development. The cyclone development time is controlled by the supply of that warm and moist air, which is rapidly reduced as the storm moves eastward away from the continent, explaining the fast recycling time of the cyclogenesis region.

5. Acknowledgments

The present work was supported by the Portuguese Foundation for Science and Technology, Grants BD/8482/2002 and POCTI/CTA/46573/2002, cofinanced by the EU through program FEDER. Suggestions made by three anonymous referees have contributed to improve the paper.

References

Bolton, D. 1980. The computation of equivalent potential temperature. *Mon. Wea. Rev.* **7**, 1046–1053.

Dal-Piva, E. 2001. Estudo de caso sobre o papel dos fluxos de calor latente e sensível em superfície em processo de ciclogénese da costa leste ocorrido na costa leste da América do Sul. Master Thesis (in Portuguese), INPE-8498-DTI/781, 162pp.

Emanuel, K. A. 1989. The finite-amplitude nature of tropical cyclogenesis. *J. Atmos. Sci.* **46**, 3431–3456.

Frederiksen, J. S. 1985. The geographical locations of Southern Hemisphere storm tracks: linear theory. *J. Atmos. Sci.* **42**, 710–723.

Gan, M. A. and Rao, V. B. 1991. Surface cyclogenesis over South America. *Mon. Wea. Rev.* **119**, 1293–1302.

Garreaud, R. D. and Wallace, J. M. 1998. Summertime incursions of midlatitude air into subtropical and tropical South America. *Mon. Wea. Rev.* **10**, 2713–2733.

James, I. N. and Anderson, D. L. T. 1984. The seasonal mean flow and distribution of large-scale weather systems in the southern hemisphere: the effects of moisture transports. *Quart. J. R. Met. Soc.* **110**, 943–966.

Kalnay, E., Kanamitsu, M., Kistler, R., Collins, W., Deaven; D. and co-authors 1996. NCEP/NCAR 40-year reanalysis project. *Bull. Am. Meteorol. Soc.* **77**, 437–471.

Marengo, J. A., Soares, W. R., Saulo, C. and Nicolini, M. 2004. Climatology of the low-level jet east of the Andes as derived from the NCEP reanalyses. *J. Climate* **17**, 2261–2280.

Peixoto, J. P. and Oort, A. H. 1992. *Physics of Climate*. American Institute of Physics, New York, 520 pp.

Possia, N. 2002. An explosive cyclogenesis over land. *Atmosféra* **15**, 1–19.

Rennó, N. O. and Ingersoll, A. P. 1996. Natural convection as a heat engine: a theory for CAPE. *J. Atmos. Sci.* **53**, 572–585.

Satyamurty, P., Nobre, C. A. and Silva Dias, P. L. 1998. Meteorology of the tropics. South America, pp 119–139, in *Meteorology of the Southern Hemisphere*. (eds D. K. Karoly and D. G. Vincent). Meteorological Monographs, 49, American Meteorological Society', Boston.

Seluchi, M. E. 1995. Diagnostico y pronostico de situaciones sinópticas conducentes a cyclogenesis sobre el este de Sudamérica. *Geofisica Internacional* **34**, 171–186.

Seluchi, M. E., and A. C. Saulo 1998. Possible mechanisms yielding an explosive coastal cyclogenesis over South America: experiments using a limited area model. *Aust. Meteor. Mag.* **47**, 309–320.

Sinclair, M. F. 1995. A climatology of cyclogenesis for the Southern Hemisphere. *Mon. Wea. Rev.* **123**, 1601–1619.

Simmonds, I. and Keay, K. 2000. Mean southern hemisphere extratropical cyclone behavior in the 40-year NCEP-NCAR reanalysis. *J. Climate* **13**, 873–885.

Trigo I. F., Davies, T. D. and Bigg, G. R. 1999. Objective climatology of cyclones in the Mediterranean region, *J. Climate* **12**, 1685–1696.

Trigo, I. F. 2005. Climatology and interannual variability of storm-tracks in the Euro-Atlantic sector: a comparison between ERA-40 and NCEP/NCAR reanalyses, Clim. Dyn., DOI 10.1007/s00382-005-0065-9.

Velasco, I. and Fritsch, M. 1987. Mesoscale convective complexes in Americas. *J. Geophys. Res.* **92**, 9591–9613.

Wilks, D., 1995. *Statistical Methods in the Atmospheric Sciences. An Introduction*. Academic Press, San Diego, 467pp.